Thermodynamic Mechanism of the Density and Compressibility Anomalies of Water in the Range -30<T(oC) <100

Makoto Yasutomi (g800002@lab.u-ryukyu.ac.jp)
University of the Ryukyus

Research Article

Keywords: Water, Density anomaly, Compressibility anomaly, Interactions between water molecules, Thermodynamic mechanism

Posted Date: September 17th, 2021

DOI: https://doi.org/10.21203/rs.3.rs-907752/v1

Noname manuscript No.
(will be inserted by the editor)

Thermodynamic Mechanism of the Density and Compressibility Anomalies of Water in the Range $-30 < T(^\circ\mathrm{C}) < 100$

Makoto Yasutomi

Received: date / Accepted: date

Abstract Compared to normal liquids, water exhibits a variety of anomalous thermal behaviors. This fact has been known for centuries. However, the thermodynamic mechanisms behind them have not been elucidated despite the efforts of many researchers. Under such circumstances, the author theoretically reproduced the measured values of the density-temperature curve at 1 atm for water above 0°C. Then, the mystery of negative thermal expansion was clarified in relation to the shapes of the intermolecular interactions. In this paper, the author develops this line of work further and presents the interactions between water molecules to simultaneously reproduce the measured values of both the density-temperature curve and the isothermal compressibility-temperature curve in the range $-30 < T(^\circ\mathrm{C}) < 100$ at 1 atm. Then, the thermodynamic mechanism that produces these thermal behaviors is clarified in relation to the shapes of the interactions between molecules. Unraveling the mystery of related phenomena in relation to the shapes of the interaction between molecules has been a traditional and fundamental method in physics since the days of Newton.

Keywords Water · Density anomaly · Compressibility anomaly · Interactions between water molecules · Thermodynamic mechanism

1 Introduction

Newton constructed calculus and mechanics to establish a method for finding the motion of a mass point from the force acting on the mass point and

Makoto Yasutomi
Department of Physics and Earth Sciences, Faculty of Science, University of the Ryukyus, Nishihara-Cho, Japan
Tel.: +81-098-895-8516
Fax: +81-098-895-8509
E-mail: g800002@lab.u-ryukyu.ac.jp

the initial conditions. This set of Newtonian mechanics has been applied to planetary motion, and it has been shown that the data on planetary motion observed by Kepler can be reproduced, assuming that Newton's universal gravitational force acts between the sun and the planet. Thus, it was discovered that Newton's universal gravitational force acts between the masses of objects.

There is no direct theoretical way to know what functional form is taken by universal gravitation. Therefore, we first assumed several different universal gravitational functional forms. From among them, the form of the universal gravitational force $F = GmM/r^2$ was determined as the functional form that successfully reproduced Kepler's observational data.

As the processing power of computers increased, Newtonian mechanics evolved into molecular dynamics. In this method, a substance consisting of innumerable molecules is approximated as a group consisting of a finite number of molecules. Then, based on Newtonian mechanics, the motion of each molecule is calculated using a computer by assuming the functional shape of the force acting between the molecules. Statistical mechanics techniques and the laws of thermodynamics can be used in this calculation to derive various thermodynamic quantities of matter.

Whether these thermodynamic quantities can reproduce the measured values for an actual substance is determined by the functional shape of the assumed intermolecular force.

It is known from thermodynamics and statistical mechanics that thermodynamic quantities in thermal equilibrium do not depend on the initial conditions of individual molecules or the path leading to the achievement of a thermal equilibrium state.

It is impossible to derive the interactions between water molecules from a basic equation such as the Schrödinger equation. At present, we can say that the functional form of an intermolecular interaction is determined as follows.

Several different types of water models have been proposed. One of them is the realistic water model, which was proposed with the main purpose of reproducing measured values with high accuracy (for example, TIP3P, TIP4P [1], SPC/E [2], TIP5P [3], TIP4P/2005 [4], and mW [5]).

In these models, for example, the oxygen atom of a water molecule is considered to be electrically neutral, and it is assumed that a Lennard-Jones potential acts between the oxygen atoms. Furthermore, the positive charge distribution and the negative charge distribution in the water molecule are represented by several point charges, and it is assumed that a Coulomb force acts between the charges. The number of point charges and the values of those charges depend on the model. There are several parameters that characterize each water model, but their values are adjusted so that the results of the model calculations and the experimental results are in good agreement (see the above references or [6]).

However, even if the thermodynamic quantities obtained by this method reproduce the related phenomenon, it is not easy to discuss the thermodynamic mechanism behind the phenomenon in relation to the shapes of the intermolecular interactions.

The simplified model or core-softened model is a method proposed to solve this difficulty and elucidate the thermodynamic mechanism behind the given phenomenon in relation to the shapes of the intermolecular interactions.

In this method, the intermolecular interactions are approximated by simple functional shapes. Thermodynamic quantities can be calculated using the Monte Carlo method or the molecular dynamics method [7], [8], [9], [10], [11], [12], [13], [14], [15], [16], [17], [18], [19].

Examples of water molecular interactions that have been proposed so far include the Lennard-Jones potential, Coulomb potential, van der Waals potential, Yukawa potential, and so on. In addition, interactions consisting of combinations of these potentials and various other forms of interactions have been proposed. However, it is not yet possible to reproduce the experimental results of water and elucidate the physics behind them.

A core-softened model for analytical calculation has been proposed in addition to numerical simulation. The self-consistent Ornstein-Zernike approximation (SCOZA) was studied by [20], [21], [22], [23], [24], [25], [26], [27], [28], and [29].

The SCOZA considers that intermolecular interactions consist of hard-core potentials and tail potentials. Various functional shapes have been proposed as tail potentials.

The author of this paper studied the thermodynamic properties of water, whose tail potentials consist of three or more Yukawa terms, using the SCOZA. He also showed that there are innumerable intermolecular interactions that can reproduce the measured values of the water density-temperature curve at 1 atm with high accuracy. He also presented many such interactions [26], [27], [28], [30].

The author went further and found the simplest interaction that could reproduce the measured values of water with high accuracy. Since the tail of this interaction consists of only two Yukawa terms, it is given by four parameters. However, one of them is used as a normalization constant, so there are only three free parameters. Therefore, it is not impossible to explore all of these parameters. In fact, the author applied this simplest interaction at 1 atm for water in the range $0< T(^\circ\mathrm{C}) <100$. He found a number of interactions that could accurately reproduce the measured values of the water density-temperature curve [31].

The core of the mystery of negative thermal expansion was explained in [32] using simple and clear laws of thermodynamics. It is summarized here. For substances with positive thermal expansion, when the temperature is kept constant, the pressure p becomes a monotonically increasing function of the density ρ on the pressure-density plane (see Fig. 2.2 of [32]). On this plane, the isotherms move to the high-pressure side as the temperature rises. The intersections of such a large number of different isotherms and a straight line with constant pressure p_0 (the red horizontal line in the previous figure) give a density-temperature curve (isobar) with respect to the pressure p_0.

From this isobar, it can be seen that the density decreases monotonically with increasing temperature. This is the simple and clear thermodynamic

mechanism of positive thermal expansion. On this p-ρ plane, if the density is kept constant, the pressure increases with temperature, so $\alpha = (\partial p/\partial kT)_\rho > 0$ (T denotes the absolute temperature and k is the Boltzmann constant). That is, $\alpha > 0$ produces a positive thermal expansion.

From the above discussion, it is immediately clear that $\alpha < 0$ produces a negative thermal expansion. That is, in a substance exhibiting negative thermal expansion, the isotherm moves to the low-pressure side in the opposite direction of the substance with positive thermal expansion as the temperature rises on the p-ρ plane. The author actually elucidated this using a water model, using the laws of thermodynamics and the techniques of statistical mechanics, in relation to the shapes of intermolecular interactions (see [32] and [27]).

However, some people still stubbornly adhere to the theory that the liquid-liquid phase transition causes negative thermal expansion. However, this is completely unconvincing. That is described in detail in the above studies. Those who advocate for the liquid-liquid phase transition theory merely state their desire to be true. These people should explain why only the liquid-liquid phase transition of water produces negative thermal expansion, contrary to the fact that all other phase transitions are accompanied by positive thermal expansion. However, that has not been done at all.

In this paper, the author presents the simplest molecular interaction that simultaneously satisfies the measured values of both the isothermal compressibility-temperature curve and the density-temperature curve for liquid water in the range $-30 < T(^\circ\mathrm{C}) < 100$ at 1 atm. Then, the mystery of the anomalous thermal behavior of isothermal compressibility is elucidated in relation to the shapes of intermolecular interactions. In addition, the difference between supercooled water and water at 0°C or higher is explained in relation to the shapes of intermolecular interactions.

Using his mechanics, during the process of theoretically reproducing Kepler's observational data, Newton discovered that there is a universal gravitational force between the masses of objects. Similarly, in this study, it is indispensable to compare the measured and theoretical values of thermodynamic quantities for water.

2 Water model

Various thermodynamic quantities can be derived from excess internal energy $u(\rho, \beta)$. This energy is defined by the following equation.

$$u(\rho, \beta) = 2\pi\rho^2 \int_0^\infty dr\ r^2 \phi(r) g(r). \tag{1}$$

Here, $\beta = 1/kT$, and $g(r)$ is a distribution function. The thermodynamic potential is clearly related to the shape of the intermolecular interaction $\phi(r)$ when compared with other thermodynamic potentials. Therefore, it is more suitable to carry out this study with $u(\rho, \beta)$ than other thermodynamic potentials.

The quantity $u(\rho, \beta)$ can be obtained by solving the following equation using the SCOZA.

$$\frac{\partial}{\partial\beta}\left(\frac{1}{\chi_{\mathrm{red}}}\right) = \rho\frac{\partial^2 u}{\partial\rho^2}. \tag{2}$$

Here, χ_{red} denotes reduced isothermal compressibility and is defined by the following equation.

$$\left(\frac{\partial\beta p}{\partial\rho}\right)_{\beta} = \frac{\beta}{\kappa\rho} \equiv \frac{1}{\chi_{\mathrm{red}}}. \tag{3}$$

Here, κ is the isothermal compressibility.

It is assumed that the intermolecular interaction $\phi(r)$ in a certain thermal equilibrium state is composed of three parts: a hard-core potential, a soft-repulsive tail, and an attractive tail. This interaction is given by the following equation.

$$\phi(r) = \begin{cases} \infty, & r < 1, \\ -\displaystyle\sum_{n=2}^{3} a_n \frac{\exp[-z_n(r-1)]}{r}, & r \geq 1, \end{cases} \tag{4}$$

Here, a_2 is a normalization constant, and a_3, z_2, and z_3 are free parameters. Additionally, the hard-core diameter σ is the unit of length, and the potential depth ε is the unit of energy (see [33] for details on the SCOZA used in this paper). To date, the author has dealt with potential tails consisting of three or more Yukawa terms [26], [27], [28], [33]. In this case, except for the normalization constant, the potential tails contain 5 or more free parameters, so it is almost impossible to survey all such tails. However, since this interaction contains only three free parameters, it is not impossible to investigate almost all shapes. Therefore, it is very convenient to carry out this research.

3 Method of calculation

If the thermal equilibrium state changes, the structure of the water molecule should change in addition to the changes in the coordination and orientation of the water molecule. Therefore, the interactions between water molecules should change constantly with changes in thermal equilibrium. The shapes of the interactions between water molecule changes with the temperature because the density is determined by specifying the temperature in the thermal equilibrium state at 1 atm. This is taken into account in this paper.

It has also been thermodynamically shown that the thermal equilibrium state does not depend on the path leading to its achievement. Therefore, at 1 atm, the shapes of the water molecule interactions at a certain temperature can be determined by the method described in the next subsection (see [33] for the detailed calculation method of the SCOZA used in this paper).

3.1 Calculation results in the range $0 < T(^\circ\mathrm{C}) < 100$

Using the diameter of a rigid sphere σ as the unit of length and the depth of the potential ε as the unit of energy, the intermolecular interactions are made dimensionless. The intermolecular interactions are determined by four parameters, a_2, a_3, z_2, and z_3. However, if we focus on z_2 and z_3, there are innumerable combinations. Nevertheless, after several trial calculations, we find that $(z_2, z_3) = (34, 35)$ is a promising combination. Therefore, if one sets $a_2 = 1$ and lets a_3 be a free parameter, for water in the temperature range of $0 < T(^\circ\mathrm{C}) < 100$ at 1 atm, it is possible to obtain a series of intermolecular interactions that can simultaneously reproduce the measured ρ-T relation and κ-T relation.

As an example, the case $a_3/a_2 = -1.0034$ is described. First, for these four parameter values, the potential depth ε is found. Dividing a_2 and a_3 by ε gives the potential normalized by σ and ε. Many isotherms can be obtained by starting from an infinite temperature and gradually lowering the temperature while keeping the shape of this normalized interaction constant.

Next, on the p-ρ plane, the isobar (ρ-T relation) is found from the intersections of the straight line of $p = p_0$ (constant) and the above isotherms. Then, the density and the temperature are normalized by the maximum values of the density and the temperature, respectively, which yields the maximum density. Given that this normalized theoretical isobar and the experimental isobar match at the point with maximum density, the values of $p_0 = 1.00$ atm, $\sigma = 3.0743$ Å and $\varepsilon = 2.077\times10^{-20}$ J are determined.

The theoretical isobar thus obtained is shown by the black dashed line in Fig. 1. Comparing the theoretical and experimental isobars (black open circles), they are, of course, consistent at 4°C. However, although there is a slight discrepancy between the two as the temperature rises, they match again in the narrow temperature range around 95.88 °C.

By changing the temperature of the theoretical isobar shown by the broken line near the latter temperature, the theoretical κ-T relation at 1 atm can be obtained (the dashed line in Fig. 2).

In exactly the same way, $(z_2, z_3) = (34, 35)$ can be kept fixed, and if one changes the value of a_3/a_2 in order to -1.0035, -1.0037, -1.0038, -1.0039, -1.00398, -1.0042 and -1.00445, the ρ-T relation and κ-T relation can be obtained, as shown by the black closed circles, in Figs. 1 and 2, respectively. The corresponding intermolecular interactions are shown by solid black lines in Fig. 3.

In Figs. 1 and 2, in the range $0 < T(^\circ\mathrm{C}) < 100$, the theoretical values (black closed circles) and the experimental values (black open circles) match with high accuracy.

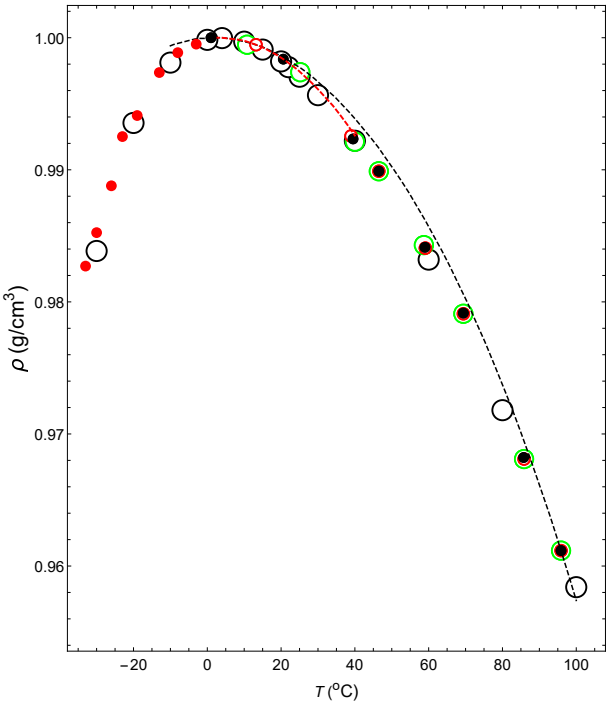

Fig. 1 The ρ-T relation at 1.00 atm. Black open circles denote the measured values of water [4], [34]. Black dashed line and black closed circles: see text. Red open circles denote the calculated values of VL1 and green open circles denote the calculated values of VL2 (see 3.2 for VL1 and VL2.). Red closed circles denote the theoretical values of supercooled water.

Table 1 The temperature dependence of the parameters that determine the intermolecular interactions of water, VL1 and VL2 at a pressure of $p = 1.00$ atm. The value of each parameter is determined only by the value of temperature T_i $(i = 1 - 8)$, regardless of the liquid type. However, the value of T_i depends on the liquid type, as shown in the Table 2.

T	$a_2(\varepsilon)$	a_3/a_2	σ(Å)	$\varepsilon(10^{-20}\mathrm{J})$
T_1	108.615	−1.0034	3.0743	2.077
T_2	108.994	−1.0035	3.0655	2.0633
T_3	109.756	−1.0037	3.0489	2.0509
T_4	110.139	−1.0038	3.0404	2.0336
T_5	110.524	−1.0039	3.0285	2.0138
T_6	110.832	−1.00398	3.0221	2.0045
T_7	111.685	−1.0042	2.9994	1.9967
T_8	112.661	−1.00445	2.9733	1.9588

3.2 The reason for the minimum value of the isothermal compressibility occurring at approximately 46°C

In the case with normal substances, the isothermal compressibility decreases monotonically as the temperature drops. Additionally, as shown in Fig. 2,

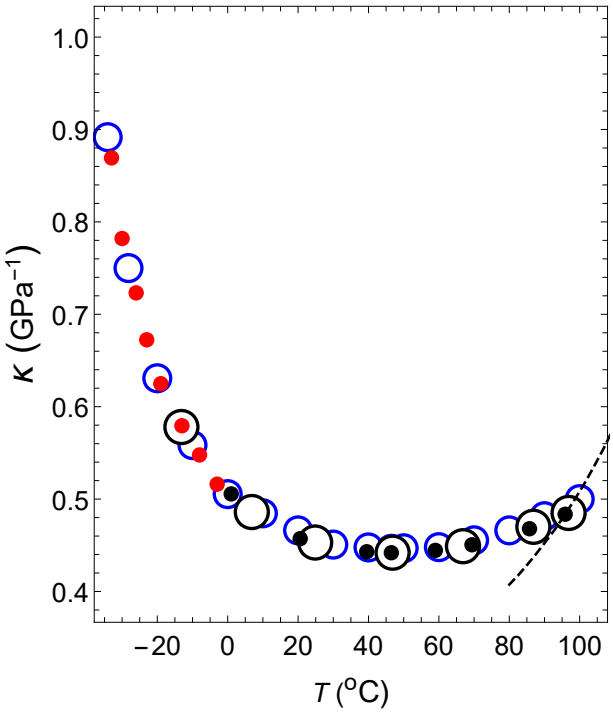

Fig. 2 The κ-T relation of water at a pressure of 1.00 atm. Black open circles: experimental values for water [35]. Blue open circles: experimental values for water [36]. Black and red closed circles: theoretical values (see text). Black dashed line (see text).

the isothermal compressibility of water decreases monotonically until approximately 46°C as the temperature drops. However, when the temperature is further lowered, it starts to increase. It has been a mystery for centuries as to why such strange behavior regarding isothermal compressibility occurs. In this subsection, we clarify this mystery in relation to the fact that the shapes of intermolecular interactions change with temperature.

When the water temperature T_i (°C) is lowered in order from $i = 1$ to $i = 8$, the shapes of the intermolecular interactions were shown in the previous section to move from right to left, as shown by the solid black line in Fig. 3. The value of T_i is shown in Table 2.

In addition, the change in the hard-core diameter σ of water with temperature is shown in Fig. 4 with black closed circles. As shown in the figure, σ is well approximated by two straight black lines with different gradients on the high-temperature side and the low-temperature side. The gradient changes rapidly around 46°C, where the isothermal compressibility κ is the minimum value. It is thought that this change creates an anomalous temperature dependence for the isothermal compressibility. To confirm this, the following two virtual liquids are considered: VL1 and VL2. Then, the temperature change of the hard-core size is compared with that of water.

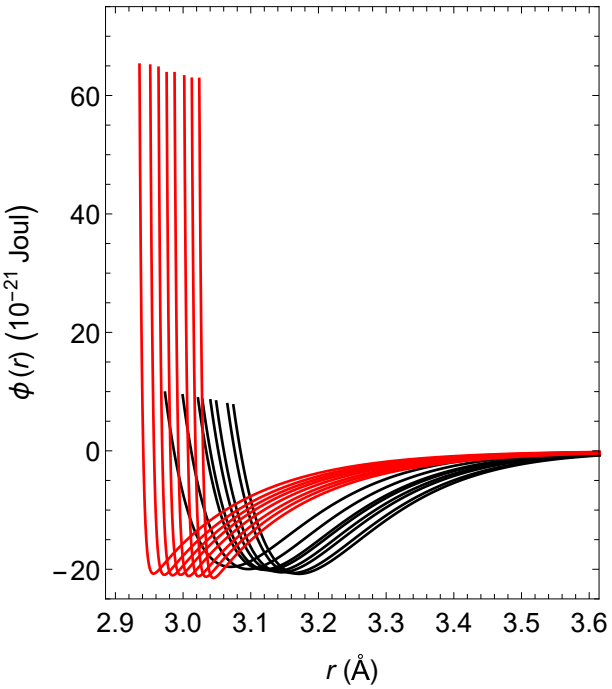

Fig. 3 Temperature dependence of the functional shapes of intermolecular interactions. The solid black lines represent the functional shapes of water, VL1 and VL2. They have the same shapes regardless of the liquid type. However, their temperature dependence differs depending on the liquid type. If one lowers the temperature shown in Tables 1 and 2 in order from T_1 to T_8, the solid black line moves from right to left. The solid red line represents the temperature dependence of the functional shapes of the intermolecular interactions for supercooled water. When the temperature is lowered in the order shown in Table 3, the red line moves from right to left.

Table 2 Values of T_i (°C) ($i = 1 - 8$) in Table 1 for water, VL1 and VL2.

liquid type	T_1	T_2	T_3	T_4
VL1	95.88	85.85	69.4	59.1
water	95.88	85.74	69.4	59.
VL2	95.88	85.74	69.4	58.7
liquid type	T_5	T_6	T_7	T_8
VL1	46.49	38.95	13.2	–
water	46.49	39.51	20.6	1.
VL2	46.49	40.	25.2	10.8

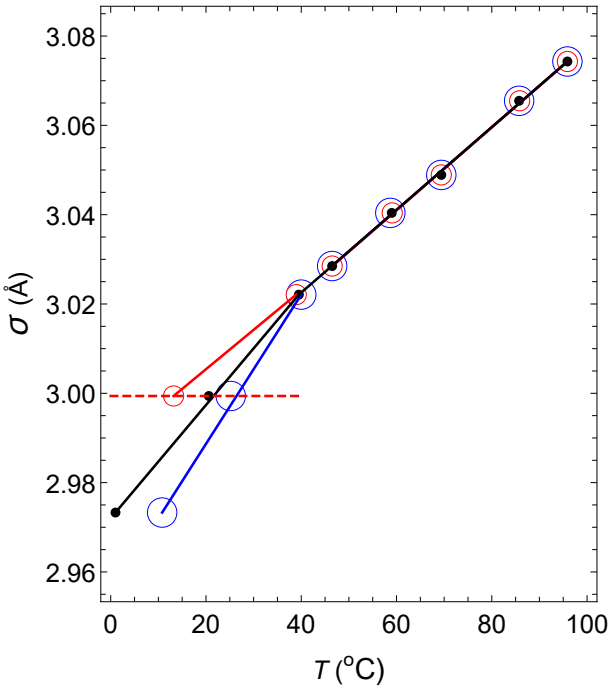

Fig. 4 The changes in the hard-core diameters σ of water, VL1 and VL2 with temperature. The diameters of water, VL1 and VL2 are shown in black, red and blue, respectively. See the text for the red dashed line.

In regard to the ρ-T relation, we assume that VL1 and VL2 exhibit the same relations as that of water. Regarding the κ-T relations of VL1 and VL2, both of them behave in the same way as water on the higher temperature side than 46°C. However, in the lower temperature region, κ of VL1 decreases monotonically as the temperature decreases (red line in Fig. 5), but κ of VL2 increases more rapidly than water (blue line) as the temperature decreases.

First, consider the case where $(z_2,\ z_3,\ a_2,\ a_3/a_2) = (34,\ 35,\ 111.685,\ -1.0042)$. The intermolecular interaction given by these parameters has the shape shown by the 7th black solid line from the right in Fig. 3. The ρ-T relation obtained by fixing this interaction and changing the temperature at 1 atm is shown by a red dashed line in Fig. 1. This red dashed line is highly consistent with the experimental values of water in the temperature range of $0 < T(°\mathrm{C}) < 40$. The κ-T relation obtained by changing the temperature on this isobar is shown by a red dashed line in Fig. 5. This red dashed line indicates that κ increases as the temperature rises. In addition, this red dashed line intersects the solid red line, solid black line, and solid blue line shown in Fig. 5 when the temperatures are 13.2, 20.6, and 25.2°C, respectively. Therefore, it can be seen that the temperature and the value of κ at this intersection give the κ-T relations of VL1, water, and VL2. The same is true for σ in the Fig. 4. The red circles, black circles, and blue circles on the red dashed line

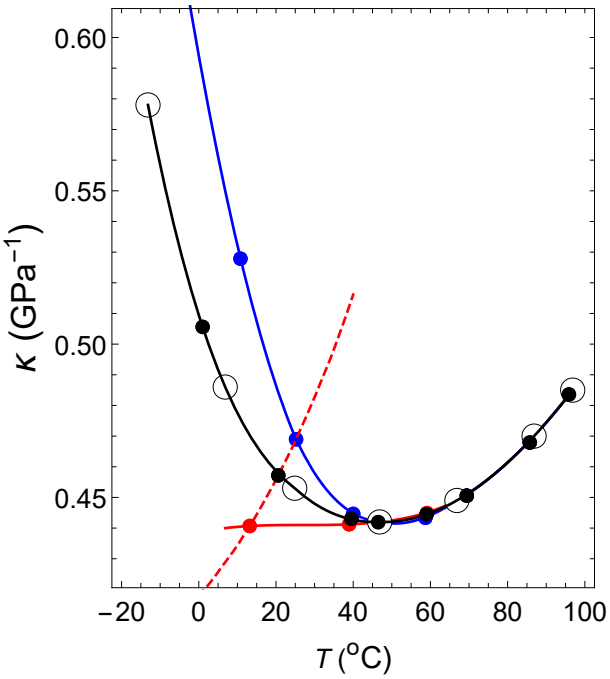

Fig. 5 The κ-T relations at a pressure of 1.00 atm for water, VL1 and VL2. Black open circles: experimental values [35]. The red, black, and blue circles and lines are the κ-T relations for VL1, water, and VL2, respectively. See the text for the red dashed line.

shown in Fig. 4 are the σ-T relations for VL1, water, and VL2, respectively. Therefore, it can be seen that this temperature dependence of σ creates an anomalous temperature dependence for the isothermal compressibility of water. Additionally, the other closed red, black, and blue circles shown in Fig. 5 are obtained in exactly the same way (see Tables 1 and 2).

3.3 Calculation results in the range $-30 < T(^\circ\mathrm{C}) < 0$

It was mentioned in the previous section that a series of intermolecular interactions are obtained as a function of temperature in the range $0 < T(^\circ\mathrm{C}) < 100$ by changing the values of a_3/a_2, as shown in Tables 1 and 2 with $(z_2, z_3) = (34, 35)$ fixed. The theoretical values of the ρ-T and κ-T relations obtained reproduce the experimental values with high accuracy.

However, if $(z_2, z_3) = (34, 35)$ remains fixed, the theoretical ρ-T relation for supercooled water below 0 °C shows that the theoretical values gradually deviate from the experimental values as the temperature drops. Therefore, we must find other value combinations that are different from those mentioned above. However, after several trial calculations, if one fixes the combination of $(z_2, z_3) = (20, 700)$ and uses a series of interactions obtained by changing the values of a_3/a_2, it turns out that both experimental κ-T and ρ-T relations

Table 3 Temperature dependence of parameters that determine the intermolecular interactions of supercooled water.

T	$a_2(\varepsilon)$	a_3/a_2	σ(Å)	$\varepsilon(10^{-20}\mathrm{J})$
−3	1.1936	−3.45	3.0239	2.147
−8	1.1939	−3.475	3.0129	2.126
−13	1.1941	−3.5	3.0017	2.118
−19	1.1944	−3.525	2.9874	2.114
−23	1.1946	−3.55	2.9757	2.093
−26	1.1949	−3.575	2.9637	2.102
−30	1.1952	−3.6	2.9515	2.093
−33	1.1955	−3.63	2.9356	2.074

can be theoretically reproduced. The combination of these values, $(z_2, z_3) = (20, 700)$, is so different that it cannot be imagined from that above. The parameters and temperatures that determine these intermolecular interactions are shown in Table 3.

The ρ-T relation and the κ-T relation are indicated in Figs. 1 and 2, respectively, with red closed circles. In each case, the theoretical results are highly consistent with the experimental values (the open black circles in Fig. 1 and open blue circles in Fig. 2, respectively).

The temperature dependence of the functional shapes of the intermolecular interactions is shown by the solid red line in Fig. 3. The functional shapes of the corresponding intermolecular interactions move from right to left in the order of decreasing temperature, as shown in Table 3. As the figure shows, the peak of the tail potential of supercooled water jumps discontinuously and dramatically around 0°C. Additionally, the σ-T relation of supercooled water is shown in Fig. 6 with red closed circles. It is also found that the value of σ jumps discontinuously around 0°C.

Both the ρ-T relation and the κ-T relation change continuously near 0°C. However, the σ-T relation and the value of the tail potential at the hard-core contact change discontinuously near 0°C. This is an interesting finding in terms of understanding the difference between supercooled water and nonsupercooled water.

4 Summary and conclusions

Thermodynamics and statistical mechanics show that the thermodynamic properties of matter are determined by the forces acting between the particles that make it up. Therefore, to fundamentally elucidate the mystery regarding the thermal behavior of matter, the topic should be discussed in relation to the shapes of particle-particle interactions. Such problem-solving methods can be said to be the most traditional and essential elucidation methods in physics since the days of Newton.

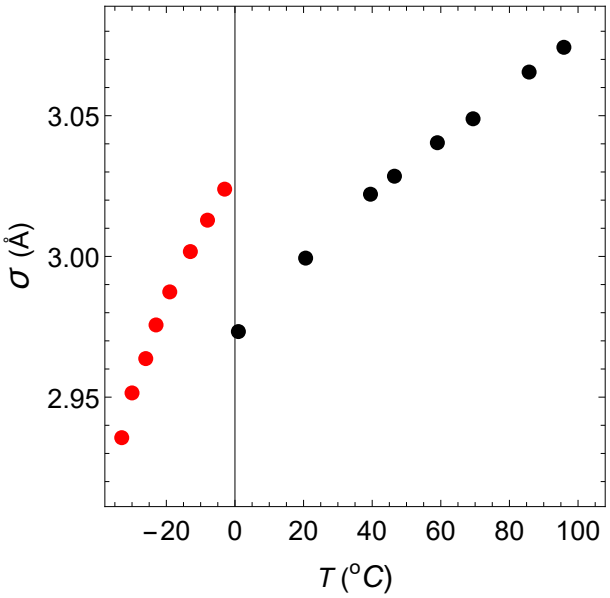

Fig. 6 The σ-T relation of water

The author discussed the mystery of the negative thermal expansion of water in [33] and [27]. He showed that $\alpha = (\partial p/\partial kT)_\rho > 0$ produces a positive thermal expansion, while $\alpha < 0$ causes a negative thermal expansion. Then, the thermodynamic mechanism was clarified in relation to the functional shapes of the interactions between water molecules.

However, some still argue that the theory that the liquid-liquid phase transition is the cause of negative thermal expansion is predominant. They merely claim that the theory is influential because they cannot think of anything else. It has been shown based on simple and clear laws of thermodynamics in [33] and [27] that this theory does not capture the essence of the phenomenon at all. It cannot be said that the liquid-liquid phase transition causes negative thermal expansion simply because the former occurs together with the latter. Whether the liquid-liquid phase transition occurs in actual water has not yet been established, but even so, it should be considered that negative thermal expansion is causing the liquid-liquid phase transition (see [33] and [27]).

In this paper, we hypothesize that the intermolecular interactions in water are constantly changing depending on the state of thermal equilibrium. This is because, in addition to the coordination and orientation of water molecules, the structures of the molecules are also considered to be constantly changing depending on the thermal equilibrium state. We also present intermolecular interactions that reproduce experimentally obtained results regarding the ρ-T relation and κ-T relation for water with high accuracy in the range $-30 < T(^\circ\mathrm{C}) < 100$. As a result, it is clarified that the anomalous behavior of the isothermal compressibility of water is produced by the changes in the shapes of

the intermolecular interactions or the changes in the diameters of the hard-core potentials with temperature.

Additionally, the maximum value of the tail of an intermolecular interaction (the value at the hard-core contact) or the diameter of the hard-core jumps up discontinuously at the melting point or freezing point of water. This is a surprising discovery, considering that the ρ-T curve and the κ-T curve are continuously changing at that point.

At present, it is impossible to derive the functional shapes of intermolecular interactions in water from basic equations such as the Schrödinger equation. The validity of the shapes must be judged by whether the assumed functional shapes can reproduce the measured values of some thermodynamic quantities of water. This is true for all water models that have been proposed to date. Newton's law of universal gravitation was discovered in this way.

The interactions between water molecules used in this paper are composed of three parts: hard-core potentials, soft repulsive tails, and attractive tails. The latter two are each represented by one Yukawa term. There are four parameters that determine the functional form of an interaction, but since one is used as a normalization constant, there are only three free parameters. Therefore, it can be said that it is not practically impossible to explore all of these functional shapes.

The author does not mention the thermal behavior of supercooled water under -30°C. Many anomalous thermal behaviors have also been found in this temperature range by experimentation or numerical simulations. Regarding the elucidation of the thermodynamic mechanism that generates such behaviors, the author believes that the method used in this paper will help elucidate them within the next few years. For that purpose, it is indispensable to compare detailed experimental values with theoretical values.

In this paper, the author presents intermolecular interactions that simultaneously reproduce the measured values of the ρ-T and κ-T relations of water. However, it should be considered that such interactions may exist in addition to those mentioned here. Nevertheless, even in that case, the author believes that the conclusions stated here will basically hold.

Finally, it is easy to imagine that the various anomalous thermal behaviors of water are thermodynamic phenomena created by the constant changes in the physical properties of water molecules themselves as the thermal equilibrium state changes.

Conflicts of interest

The author declares that he has no conflicts of interest.

References

1. Jorgensen, W. L., Chandrasekhar, J., Madula, J. D., Impey, R. W., and Klein, M. L. Comparison of simple potential functions for simulating liquid water, *J. Chem. Phys.*, **79**,

926 (1983).
2. Berendsen, H. J. C., Grigera, J. R., and Straatsma, T. P. The missing term in effective pair potentials, *J. Phys. Chem.*, **91**, 6269 (1987).
3. Mahoney, M. W., and Jorgensen, W. L. A five-site model for liquid water and the reproduction of the density anomaly by rigid, nonpolarizable potential functions. *J. Chem. Phys.*, **112**, 8910 (2000).
4. Abascal, J. L. F., and Vega, C. A general purpose model for the condensed phases of water: TIP4P/2005, *J. Chem. Phys.*, **123**, 234505 (2005).
5. Molinero, V., and More, E. B. Water modeled as an intermediate element between carbon and silicon, *J. Phys. Chem. B*, **113**, 4008 (2009).
6. Yasutomi, M., The Physics of Liquid Water, 14-15. Jenny Stanford Publishing, Singapore (2021)
7. Caballero, J. B., and Puertas, A. M. Density anomaly and liquid-liquid transition from perturbation theories, *Phys. Rev. E*, **74**, 051506 (2006).
8. Fomin, Y. D., Tsiok, E. N., and Ryzhov, V. N. Inversion of sequence of diffusion and density anomalies in core-softened systems, *J. Chem. Phys.*, **135**, 234502 (2011).
9. Gibson, H. M., and Wilding, N. B., Metastable liquid-liquid coexistence and density anomalies in a core-softened fluid, *Phys. Rev. E*, **73**, 061507 (2006).
10. Gribova, N. V., Fomin, Y. D., Frenkel, D., and Ryzhov, V. N. Water like thermodynamic anomalies in a repulsive-shoulder potential system, *Phys. Rev. E*, **79**, 051202 (2009).
11. Jagla, E. A., Low-temperature behavior of core-softened models: water and silica behavior, *Phys. Rev. E*, **63**, 061509 (2001).
12. Lomba, E., Almarza, N. G., Martin, C., and McBridge, C. Phase behavior of attractive and repulsive ramp fluids: integral equation and computer simulation studies, *J. Chem. Phys.*, **126**, 244510 (2007).
13. Malescio, G., Prestipino, S., and Saija, F. Anomalous melting and solid polymorphism of a modified inverse-power potential, *Mol. Phys.*, **109**, 2837-2844 (2011).
14. Oliveira, A. B. De, Netz, P. A., and Barbosa, M. C., An ubiquitous mechanism for water-like anomalies. *EPL*, **85**, 36001 (2009).
15. Prestipino, S., Saija, F., and Malescio, G. Anomalous phase behavior in a model fluid with only one type of local structure, *J. Chem. Phys.*, **133**, 144504 (2010).
16. Sadr-Lahijany, M. R., Scala, A., Buldyrev, S. V., and Stanley, H. E., Liquid-State Anomalies and the Stell-Hemmer Core-Softened Potential, *Phys. Rev. Lett.*, **81**, 4895 (1998).
17. Wilding, N. B., and Magee, J. E., Phase behavior and thermodynamic anomalies of core-softened fluids, *Phys. Rev. E*, **66**, 031509 (2002).
18. Yan, Z., Buldyrev, S. V., Giovambattista, N., and Stanley, H. E., Structural Order for One-Scale and Two-Scale Potentials, *PRL*, **93**, 130604 (2004).
19. Yan, Z., Buldyrev, S. V., Kumar, P., Giovambattista, N., and Stanley, H. E., Correspondence between phase diagrams of the TIP5P water model and a spherically symmetric repulsive ramp potential with two characteristic length scales, *Phys. Rev. E*, **77**, 042201 (2008).
20. Betancourt-Cárdenas, F. F., Galicia-Luna, L. A., Benavides, A. L., Ramirez, J. A., and Sch`oll-Paschinger, E., Thermodynamics of a long-range triangle-well fluid, *Mol. Phys.*, **106**, 113 (2008).
21. Pini, D., Stell, G., and Wilding, N. B., A liquid state theory that remains successful in the critical region, *Mol. Phys.*, **95**, 483-494 (1998).
22. Pini, D., Stell, G., and Dickman, R., Thermodynamically self-consistent theory of structure for three-dimensional lattice gases, *Phys. Rev. E*, **57**, 2862 (1998).
23. Schöll-Paschinger, E., Self-consistent Ornstein-Zernike approximation for the Sogami-Ise fluid, *J. Chem. Phys.*, **120**, 11698 (2004).
24. Schöll-Paschinger, E., Vapor-liquid equilibrium and critical behavior of the square-well fluid of variable range: A theoretical study, *J. Chem. Phys.*, **123**, 234513 (2005).
25. Yasutomi, M., A self-consistent Ornstein-Zernike approximation for a fluid with a screened power series interaction, *J. Chem. Phys.*, **133**, 154115 (2010).
26. Yasutomi, M., Interparticle interactions between water molecules, *Front. Phys.* **2**, 64 (2014).
27. Yasutomi, M., Thermodynamic mechanism of the density anomaly of liquid water, *Front. Phys.*, **3**, 8 (2015).

28. Yasutomi, M., Which shape characteristics of the intermolecular interaction of liquid water determine its compressibility, *Front. Phys.*, **4**, 21 (2016).
29. Yasutomi, M., The Physics of Liquid Water, 48-59, Jenny Stanford Publishing, Singapore (2021).
30. Yasutomi, M., The Physics of Liquid Water, pages 19, 24, and 138, Jenny Stanford Publishing, Singapore (2021).
31. Yasutomi, M., The Physics of Liquid Water, 137-140, and 138, Jenny Stanford Publishing, Singapore (2021).
32. Yasutomi, M., The Physics of Liquid Water, 8-10, and 18-22, Jenny Stanford Publishing, Singapore (2021).
33. Yasutomi, M., The Physics of Liquid Water, Jenny Stanford Publishing, Singapore (2021).
34. Lide, D. R., CRC Handbook of Chemistry and Physics (70th Edn.), CRC Press, Boca Raton (FL), (1990).
35. Pi, H. L., Aragones, J. L., Vega, C., Noya, E. G., Abascal, J. L. F., Gonzalez, M. A., and McBride, C., Anomalies in water as obtained from computer simulations of the TIP4P/2005 model: density maxima, and density, isothermal compressibility and heat capacity minima, *Mol. Phys.*, **107**, 365-374 (2009).
36. Chaplin, M., http://www1.lsbu.ac.uk/water/explan2.html.